*Journal of Structural Geology*, Vol. 4, No. 2, pp. 137 to 149, 1982.
Printed in Great Britain

0191-8141/82/020137-12 $03.00/0


# Deformation mechanisms in some cover thrust sheets from the external French Alps

A. BEACH*

Department of Geology, The University, P.O. Box 147, Liverpool L69 3BX, England

(*Received* 25 *June* 1981; *accepted in revised form* 10 *December* 1981)

**Abstract**—Rocks from two parts of the Ultradauphinois Zone of the external French Alps have been examined, and the mechanisms by which they were deformed have been assessed from petrographic data. Jurassic and Triassic limestones deformed by pressure solution, dissolving non-ferroan-calcite and precipitating ferroan-calcite. Calcite pressure shadows are usually less elliptical in shape than pyrite pressure shadows, and grain boundary sliding is therefore thought to have played a significant role. Eocene rocks deformed by a variety of mechanisms. Limestones show mylonitic textures, whereas limestone conglomerates with a quartz–sandstone matrix deformed by pressure solution of calcite and grain boundary sliding of quartz. A model for enhanced diffusion of silica along mica seams is proposed to account for planar quartz–mica boundaries. Greywackes deformed by incongruent pressure solution, involving the metamorphic reaction of feldspar to mica and quartz, coupled with the replacement of feldspar by calcite.

## INTRODUCTION

IN THE area of the external French Alps to the north of the Pelvoux basement massif, referred to by Debelmas & Lemoine (1970) and Debelmas & Kerckhove (1980) as the Ultradauphinois Zone, two imbricated zones of cover sequences have been described (Beach 1981a). The cover thrust structures have been correlated across lateral ramps with basement structures in the Pelvoux massif (Beach 1981a, b). The cover rocks comprise a sequence of thin Trias (largely dolomitic), Jurassic muddy limestones and marls, and Eocene conglomerates and flysch (Fig. 1). The sequence is strongly deformed in the thrust sheets (Beach 1981c), and it is the purpose of this paper to present an interpretation of the mechanisms of deformation, based on petrographic study of the deformed rocks. Bernard (1978) and Bernard *et al.* (1977) suggest that $P$, $T$ conditions during the formation of syntectonic veins in the area were approximately 2–2.5 kb, 250°C. The studies of Kerrich *et al.* (1977) indicate that pressure solution may be the dominant mechanism of deformation under these conditions.

There is considerable evidence in the field that pressure solution played a significant role in the deformation, e.g. pressure shadows, stylolites, infills between segments of extended belemnites, syntectonic veins (cf. Durney 1972). Evidence for plastic deformation is less forthcoming in the field (cf. Ramsay 1981). Pebbles in the conglomerates at the base of the Eocene succession have often undergone a considerable shape change by internal strain. However, it is only in the overlying thrust sheets of the internal nappes (sub-Briançonnais zone) that plastic deformation of grains is commonly seen (e.g. deformed oolitic limestones).

The descriptions below are divided into three sections, covering (a) deformation in the Triassic–Jurassic sequence, (b) deformation in the conglomerates at the base of the Eocene succession and (c) deformation in the sandstones of the Eocene flysch succession (Fig. 1).

## DEFORMATION IN TRIASSIC AND JURASSIC ROCKS

Detachment of the cover thrust sheets forming the two imbricate stacks of the Ultradauphinois Zone occurred at the transition from Trias to Lower Lias. Isolated slabs or lozenges of Triassic rock are commonly found along the base of a thrust sheet, overlain by Jurassic rock making up the sheet itself. The Triassic material may be limestone, dolomite, cargneule (Warrak 1974), and in the north of the region, gypsum.

In the field, the dolomites appear little deformed by ductile strains, though they may be fractured and veined. In thin section they appear as equigranular, interlocking grain mosaics with little evidence of deformation either by pressure solution or intracrystalline strain. In contrast, the limestones have been deformed by pressure solution. Using carbonate stains, it is found that non-ferroan-calcite grains of the limestone have developed pressure shadow overgrowths of ferroan-calcite (Figs. 2a and 3a). The pressure shadow is normally a single crystal in crystallographic continuity with the host grain.

Jurassic rocks range from impure limestones through muddy limestones to marls and pelitic shales. The limestones are generally fine grained, commonly with grain diameters from 10 to 50 $\mu$m. They contain a variable proportion (up to 20%) of larger grains recognisable as fossil fragments, with diameters ranging up to 100–500 $\mu$m. The finite strain varies throughout the Jurassic rocks making up the thrust sheets, and the following observations can be made.

* Present address: Exploration Geology, British National Oil Corporation, 150 St. Vincent St., Glasgow, Scotland.

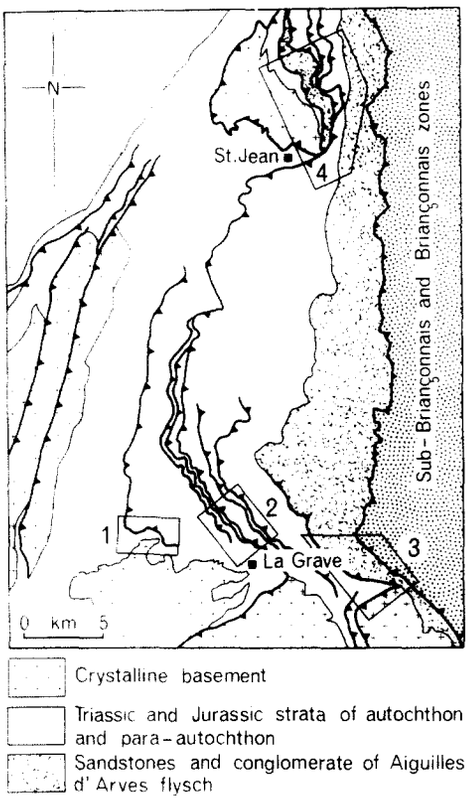


Fig. 1. Simplified geological map of the Ultradauphinois Zone showing principal rock groups studied, the main thrust units and the areas of pre-Triassic crystalline basement. The areas in which rocks have been studied are indicated: (1) the deformed L. Mesozoic autochthon, resting on crystalline basement; (2) the La Grave thrust belt of Trias and L. Jurassic; (3) the deformed Aiguilles d'Arves flysch structurally overlying the top of the La Grave thrust belt and (4) the St. Jean thrust belt of Triassic, L. Jurassic and Eocene rocks, overlying crystalline basement and overlain by deformed Aiguilles d'Arves flysch.

(i) There is no systematic difference in grain size between limestones showing a low deformation and those showing a high deformation; in both, the grain size varies in the range given above.
(ii) In the little deformed limestones, there is a high proportion of non-ferroan-calcite and only a small amount of ferroan-calcite; the reverse is true for the strongly deformed limestones.
(iii) Pressure shadows are particularly clearly developed on fossil fragments where ferroan calcite overgrows non-ferroan-calcite; the overgrowth may be in optical continuity with the host grain (Fig. 3a), or it may consist of an aggregate of small grains (Fig. 2b).
(iv) The non-ferroan-calcite segments of extended belemnites are overgrown in crystallographic continuity by pressure shadows of ferroan-calcite (Fig. 2c).
(v) The fossil fragments are generally single crystals of calcite showing marginal pressure solution, with little evidence of internal strain (twinning, undulatory extinction), in rocks of low finite strain; in more deformed rocks, some now consist of an equigranular aggregate.
(vi) The matrix grains of deformed limestones are generally elongate in the trace of the cleavage, though the grain shape only rarely approaches the eccentricity of the measured strain ellipse from the same rock. This is particularly true in strongly deformed rocks.

Pressure solution of non-ferroan-calcite and precipitation of ferroan calcite played an important role in the deformation of the Jurassic limestones. It is suggested that the iron is supplied by the breakdown of small grains of siderite which can be found in many of the little deformed rocks, but rarely in those that show strong deformation. In addition, the development of a strong preferred orientation of illite–muscovite is seen in the more muddy limestones. Some of the evidence above suggests that much of the calcite recrystallised during deformation. The recrystallised calcite is usually a ferroan variety. The role of grain boundary sliding and dislocation creep in the deformation is difficult to assess from the observed textures. The grain refinement and the core and mantle textures described by White (1976) as characteristic of dislocation creep in quartzites are not seen in the limestones under discussion (cf. Schmid *et al.* 1981). On the other hand, the difference, noted above, between finite strain in a rock (recorded by extended belemnites or pyrite pressure shadows) and the grain shape/deformation is interpreted to indicate that grain boundary sliding did play a significant role during deformation (Borradaile 1981).

Considering now the pressure solution part of the deformation mechanism alone, it is clear that the calcite shows a solid solution change in composition during pressure solution. Most papers on pressure solution consider only solution and deposition of the same composition (e.g. Paterson 1973, Durney 1976). Durney shows how chemical potential gradients are related to variations in normal stress around grain boundaries and in mean stress around larger more competent objects in a matrix (cf. Gratier 1979). The relation derived by Gibbs (see Paterson 1973) gives the chemical potential of the solute in a solution under conditions of local equilibrium between stressed solid and solution. The local equilibrium value of this chemical potential will vary from one site to another through variations in stress and grain boundary orientation. Pressure solution of one composition and deposition of another in a solid–solution system is a record of these variations in chemical potential. No data are available at present on the compositions of and compositional variations between the ferroan-calcite overgrowths. It is necessary that further research be directed towards evaluating phase diagrams in terms of chemical potential–composition–stress for simple minerals such as calcite which show solid solution changes in composition during deformation by pressure solution.

## DEFORMATION IN EOCENE CONGLOMERATES AND INTERBEDDED ROCKS

Rocks of Eocene age rest unconformably across Jurassic, Triassic and basement in the area under discussion (Barbier 1963, Beach 1981a, see Fig. 1). The basal Eocene shales form the roof decoupling zone to the La Grave duplex of Jurassic thrust sheets, while the unconformity

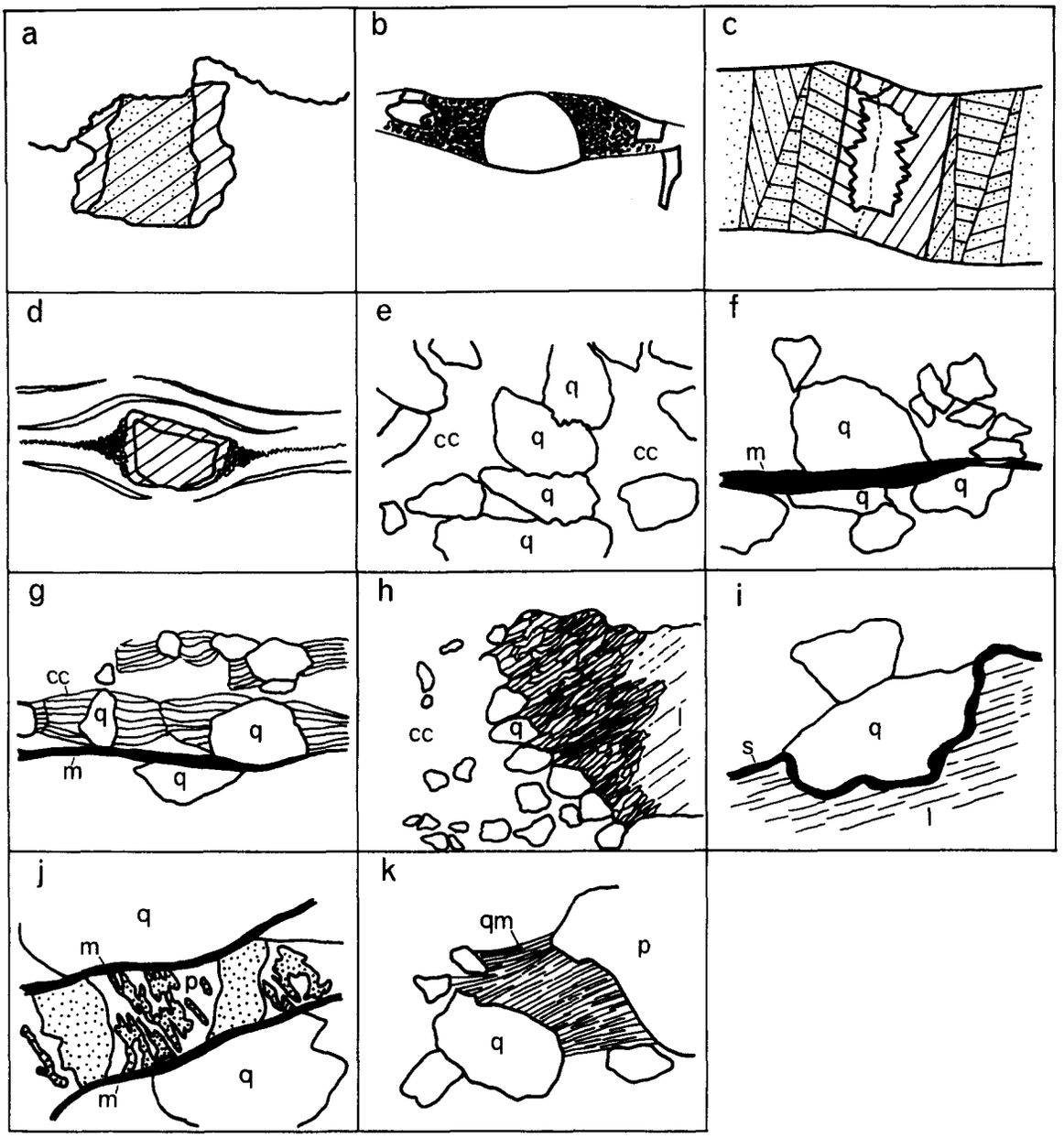


Fig. 2. (a) Plate of non-ferroan-calcite (stippled) in a limestone with oriented overgrowths of optically continuous ferroan-calcite. Twins pass continuously from host to overgrowth. Solution of both host grain and overgrowth occurs against a stylolitic seam. Field width 1 mm. (b) A circular fossil fragment of non-ferroan-calcite showing marginal truncation by pressure solution, and no internal distortion. The pressure shadow area is a much finer grained aggregate of ferroan-calcite. Field width 2 mm. (c) Part of an extended belemnite, showing the original belemnite skeleton of non-ferroan and transversely disposed calcite crystals as stippled areas. The volume between separated parts of the skeleton is filled by ferroan-calcite and quartz. Ferroan-calcite grows in optical continuity with the host, and twins pass continuously from one to the other. The quartz is located centrally in the extension zone, and shows a fine median septum. Quartz–calcite boundaries are planar surfaces reminiscent of compromise boundaries. Field width 1 cm. (d) Plate of non-ferroan-calcite forming a porphyroclast in a fine sparry limestone. The rim of non-ferroan-calcite overgrowing the plate in optical continuity may be of diagenetic origin. A tail of fine grained calcite grains is developed from each side of the porphyroclast, the grain size gradually decreasing away from this. Field width 2 mm. (e) Quartz grains (q) showing sutured contacts and set in a matrix of ferroan calcite (cc). Field width 2 mm. (f) Quartz grains (q) showing planar contacts against a mica seam (m). Field width 2 mm. (g) Well developed pressure shadows of fibrous ferroan-calcite (cc) on quartz grains (q), the latter showing planar contacts where against a mica seam (m). Field width 2 mm. (h) Part of a limestone fragment (l) in a conglomerate, the limestone showing a well developed grain elongation fabric. Quartz grains (q) around the limestone do not show this shape fabric. They are surrounded by ferroan-calcite (cc). Pyrite pressure shadows in the calcite–quartz matrix (not shown) have a similar shape to the harmonic mean of the limestone fragments. Field width 2 mm. (i) Quartz grain (q) pitted into the margin of a limestone fragment (l) with an opaque stylolite seam (s) along its margin and truncating the grain shape fabric in the limestone (indicated by the lines). Field width $\frac{1}{2}$ mm. (j) Greywacke with detrital plagioclase (p) partially replaced by ferroan-calcite (stippled) and bounded by white mica (m) in contact with detrital quartz grains (q). Field width 1 mm. (k) Greywacke with fibrous quartz–mica pressure shadow overgrowth (qm) between detrital quartz (q) and plagioclase (p). Field width 1 mm.

and Eocene strata are repeated in the St. Jean duplex to the north (Beach 1981a). Deformation is continuous across the boundary from Mesozoic to Eocene in these areas. Similar types and orientations of fabric and finite strains are found in both Mesozoic and Eocene rocks (cf. Beach 1981c). Limestones, calcareous shales, quartz sandstones and conglomerates are interbedded and vary in thickness and extent in the lowest part of the Eocene succession (Barbier 1963, Bravard & Gidon 1979). The conglomerates contain a variety of pebble types from the basement, Trias, Jurassic and slumped Eocene limestones, with a matrix that varies from muddy to sandy. A number of rocks have been examined from the thrust sheet deformed in the St. Jean duplex (Beach 1981a) and these are described here. Conglomerates containing limestone fragments set in a largely quartz sandstone matrix are present, and an interesting contrast in the mechanism of deformation in these rock types has been found.

Continuous limestone beds in this sequence frequently show fluxion structure and porphyroclastic texture characteristic of mylonites (Higgins 1971) produced by grain refinement processes during dislocation creep (White 1976). Clearly there is no way of eliminating the possibility that these limestones were deposited as alternations of fine and coarse sparry calcite containing larger fossil fragments (e.g. echinoid plates). However, in support of a deformation mechanism dominated by dislocation creep, the following observations are cited.

(i) The large calcite plates (up to 2 mm long) commonly have overgrowths of calcite (non-ferroan) which have been drawn out and recrystallised to equant grain aggregates where the grain size gradually decreases away from the host grain (Fig. 2d).

(ii) Some grains with concentric oolitic structure are now ellipsoidal in shape.

(iii) The grain size in the matrix varies continuously along the length of layers from 60 to 70 $\mu$m where the layers are thickest to 10 $\mu$m where the layers are thinnest. The calcite remains a non-ferroan variety.

(iv) Truncated margins to large calcite plates and stylolitic grain contacts are uncommon.

The deformation mechanism of these limestones is thus interpreted to be different from that in the Jurassic limestones described above. In contrast, interbedded sandstones of the Eocene sequence are seen to have deformed largely by pressure solution. These sandstones consist of quartz grains (commonly up to 1 mm in diameter) with little or no detrital feldspar or carbonate, and a small, variable proportion of clay seams. The following features are relevant to an interpretation of the deformation mechanism of these rocks.

(i) Quartz grains commonly show undulose extinction and some show subgrain formation, but recrystallisation is not seen.

(ii) Quartz grains in contact usually show stylolitic pressure solution contacts (Fig. 2e). Only very small amounts of quartz overgrowth are seen where original grain boundaries are occasionally marked by a line of fine dust inclusions.

(iii) Quartz grains are truncated by pressure solution to produce planar contacts against clay/mica seams (Fig. 2f and 3c).

(iv) Oriented pressure shadow overgrowths on quartz consist almost entirely of ferroan calcite (Fig. 2g), which may make up to 40% of the deformed rock. There are too few calcite grains in the sandstones for the pressure shadow growth to have been derived by pressure solution within the sandstone beds.

There is a gradation from these sandstone beds through to conglomerates consisting of subangular pieces of fine sparry limestone, which may be several cm long, in a quartz–sandstone matrix. The following observations are made:

(i) Little deformed quartz grains are set in a matrix of ferroan calcite forming pressure shadow overgrowths, similar to those in Fig. 2(g).

(ii) Quartz grains in contact show some pressure solution where mica seams are present. Clean contacts show only a little suturing and strongly undulose extinction within the quartz grains around the contacts.

(iii) The limestone fragments are fine and even grained with a grain shape fabric; the grains are commonly 50 $\mu$m by 15 $\mu$m. Some longer calcite ribbons up to 300 $\mu$m long are seen which consist of several subgrains of very similar optic orientation. This fabric does not pass into the sandstone matrix (Fig. 2h).

(iv) The matrix often contains framboidal pyrites with well developed pressure shadows. The strain judged from these (e.g. $X/Z = 20/1$) is very similar to that estimated from the harmonic mean (Lisle 1977) of the limestone pebble shapes in the same specimen. This is much greater than the shape of pressure shadows around quartz grains (approximately 2–3/1), but similar again to the shape of those calcite ribbons, referred to above, preserved in the deformed limestone fragments.

(v) Quartz grains are heavily pitted into the margins of limestone fragments (Fig. 2i). The stylolitic surfaces separating the two truncate the grain shape fabric in the limestone.

A rather complex interplay of deformation mechanisms is suggested by the above observations. Whilst dislocation mechanisms may dominate in the continuous limestone beds, they are subordinate to pressure solution in the limestone fragments in the conglomerates, where elongate ribbons, recrystallised to some extent through subgrain formation, are seen. Pressure solution of quartz grains does not appear to have been important, even though locally high stresses may have existed at grain contacts where strong undulose extinction is observed. The growth of pressure shadows of calcite on quartz grains does not measure the total strain in the rock as recorded by either pyrite pressure shadows or the pebble shapes. It is thus suggested that grain boundary sliding may have played an important role in the deformation of the sandstone matrix of these conglomerates (Borradaile 1981).

It is interesting to note that pressure solution of quartz grains during the deformation of these rocks is most marked where these grains are in contact with mica seams (Fig. 2f and 3c, cf. Fig. 3d). This phenomenon has been observed many times by workers on pressure solution (e.g.

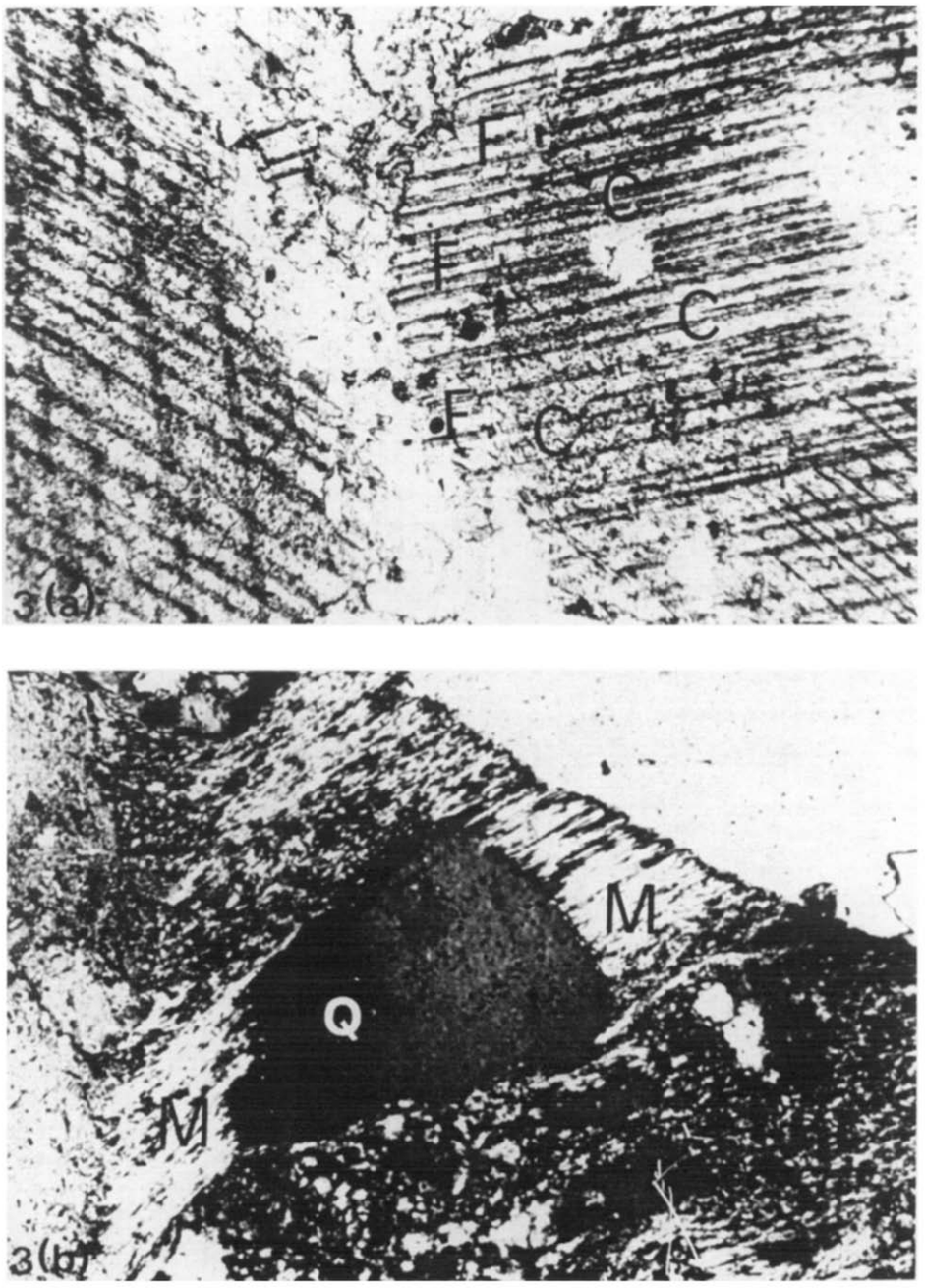


Fig. 3. (a) Overgrowth of ferroan-calcite (F) on calcite grain (C) in a Jurassic limestone. Field width 0.1 mm. (b) Oriented overgrowth of mica and quartz (M) on detrital quartz grain (Q) in a sample of Aiguilles d'Arves greywacke. Field width 0.1 mm.

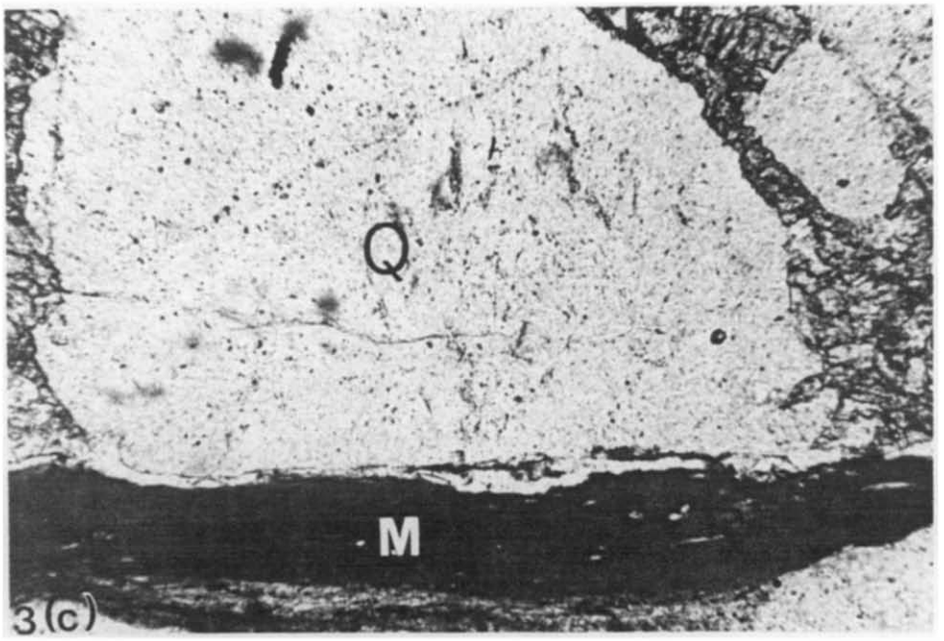


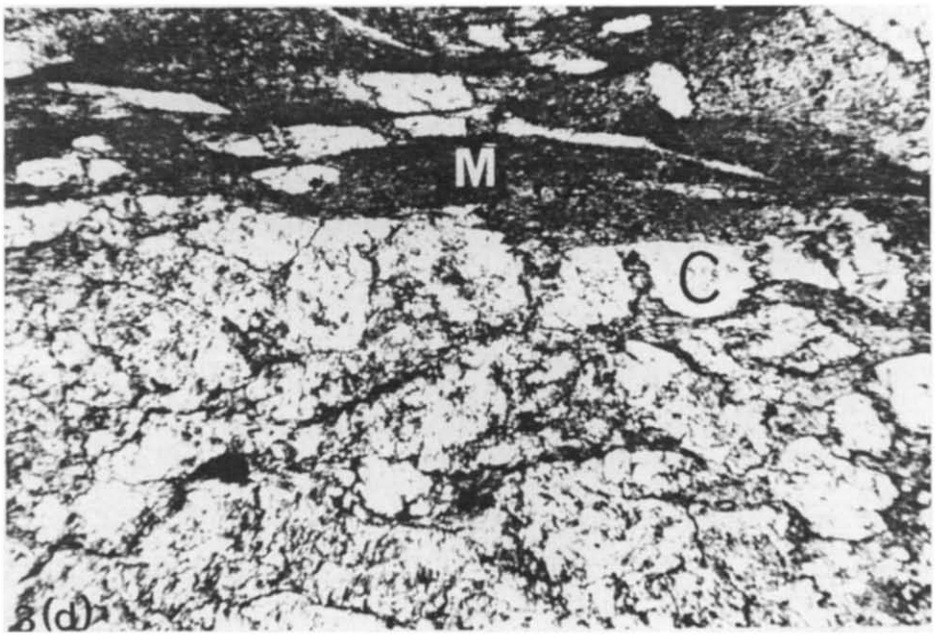


Fig. 3 (cont.).

(c) Planar pressure solution contact of detrital quartz grain (Q) against a mixed clay–mica seam (M), from a artz–sandstone in the Aiguilles d'Arves flysch succession. Field width 0.5 mm. (d) Planar pressure solution contacts between calcite grains (C) and mica–clay seams (M) in a Jurassic limestone. Field width 0.5 mm.

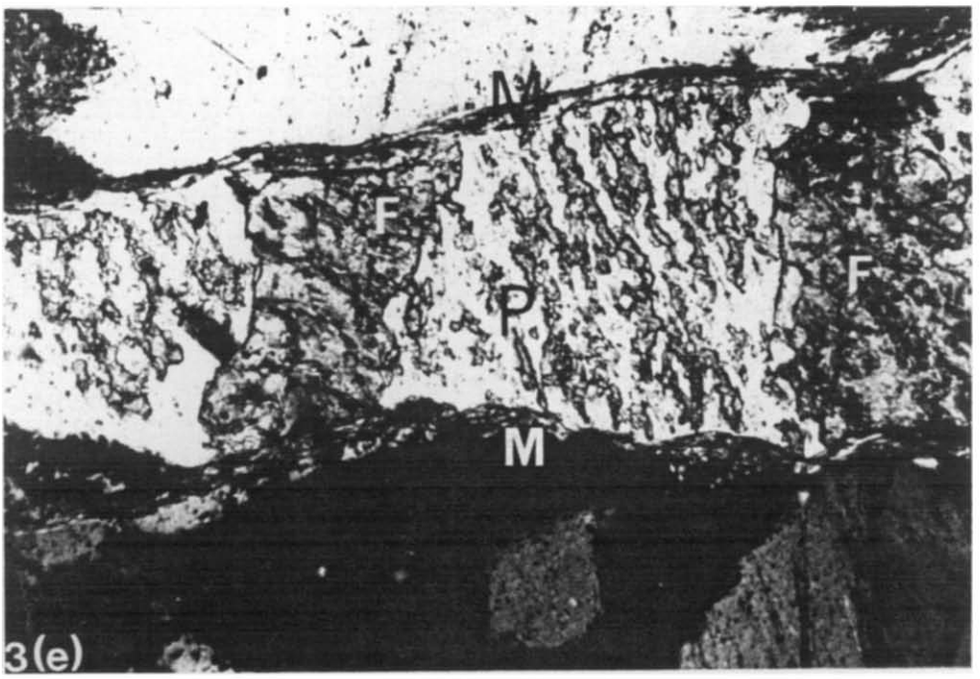


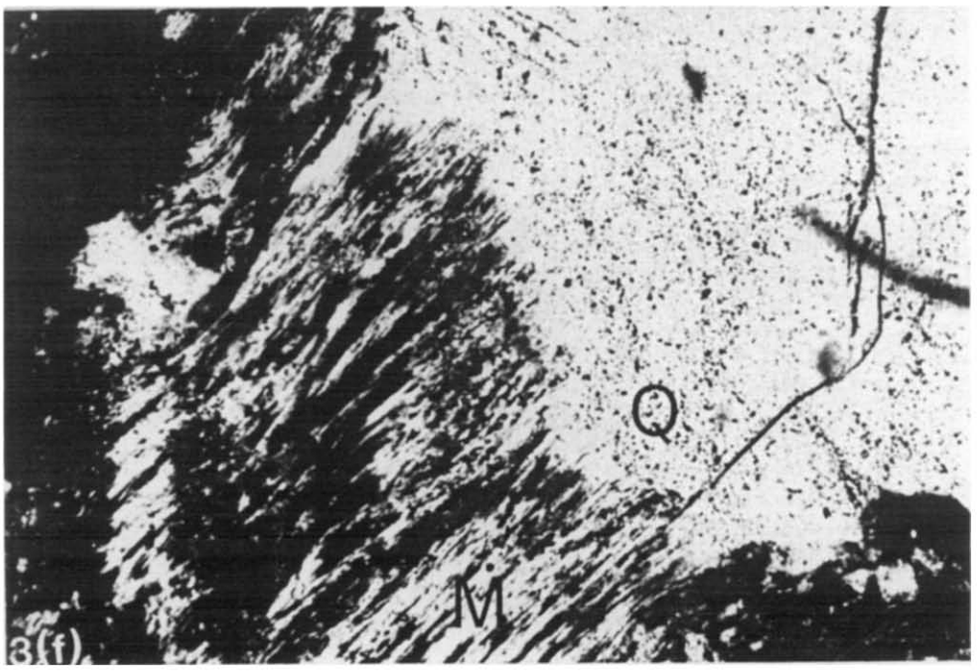


Fig. 3. (cont.).

(e) Detrital plagioclase grain (P) partially replaced by ferroan-calcite (F) and with a marginal growth of white mica (M) in a sample of Aiguilles d'Arves greywacke. Field width 0.5 mm. (f) Fibrous intergrowth of quartz and mica (M) forming an oriented pressure-shadow overgrowth on a detrital quartz grain (Q) in a sample of Aiguilles d'Arves greywacke. Field width 0.1 mm.

Heald 1955, 1959, Durney 1976, Kerrich 1977, Robin 1979). However, no quantitative measurements on relative amounts of dissolved material, and no microchemical mechanism has been proposed to explain the observations. Rutter (1976) and Durney (1976) present rate equations for deformation by pressure solution, where the variables are diffusion coefficient, grain size, normal stress and temperature. The difference between pressure solution at quartz–quartz contacts and that at quartz–mica contacts is attributed to differences in the magnitude of the diffusion coefficient. Grain size is fairly uniform in the samples examined, and no significant variation in normal stress or temperature from one grain to another is anticipated. Diffusion is considered to be the rate-determining step in metamorphic processes (Fisher & Elliott 1974, Fisher 1978). Two factors which will affect the rate of grain boundary diffusion during the pressure solution of the quartz grains are the nature and width of the grain boundary and the activation energy for diffusion (Lacy 1965, McLean 1965, Rutter 1976, McClay 1977). A model of diffusion at quartz–mica boundaries is now proposed.

Little is known of the structure of grain boundaries in metamorphic rocks, and in his treatment of pressure solution, Rutter (1976) used a grain boundary width of twice the Burgers vector of the minerals concerned (quartz and calcite). Water molecules present along such boundaries will be oriented and adsorbed onto the grain surface by interaction of the electrostatic forces of the water dipole and residual grain–lattice surface charges. It is suggested that it is the degree of ordering along the boundary that assists diffusion, primarily through lowering the activation energy for diffusion. In particular, mica boundaries are dominated by 001 cleavage surfaces formed along the planes of the 12-fold co-ordinated alkali atoms. The residual surface charge will attract water dipoles and the planar boundary will be solvated with a semi-ordered water layer (Fig. 4a). Silica molecules enter the grain boundary 'solution' as $H_4SiO_4$ molecules, and these can also adopt a preferred configuration on the mica surface through the formation of loose hydrogen bonds between the $H_2O$ of the $H_4SiO_4$ and the mica surface (Fig. 4b). The units involved have a similar size. The separation of two oxygens along the edge of a silica tetrahedron is approximately 2.5 Å and the separation of oxygen atoms on the 001 mica surface is approximately 3 Å. Under the influence of a chemical potential gradient along the mica surface, diffusion of the silica group will occur by weakening of the electrostatic attraction between Si and one of the water molecules solvating the silica group, rotation of the silica group, and transfer of electrostatic attraction to an adjacent oriented water molecule (Figs. 4b & c). Diffusion is thus reduced to a two-dimensional translation on a mica surface. The activation energy for diffusion is that needed for transfer of the electrostatic attraction. It will be considerably less than for diffusion along a less structurally compatible grain boundary, where not only three-dimensional rotations of molecules may be involved, but where transfer of electrostatic attraction is more difficult to achieve. Thus, a mechanism for an increased rate of pressure solution at quartz–mica contacts through a lowering of the activation energy for the diffusion is proposed.

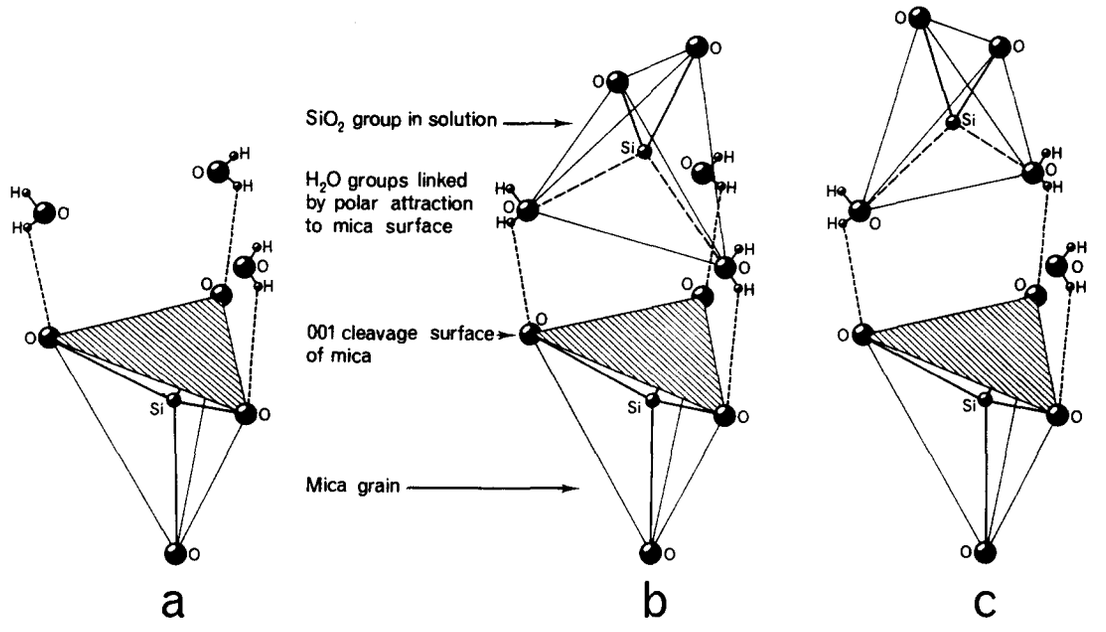


Fig. 4. (a) One upward facing silica tetrahedron of the muscovite tetrahedral layer; the mica cleavage surface is parallel to the basal plane of the tetrahedron. This surface dominates the grain boundaries of oriented mica flakes at pressure solution interfaces. No charge balancing $K^+$ atoms are shown; instead oriented water molecules are held at the mica surface by polar attraction (short-dashed lines). (b) An $SiO_2$ group in solution is oriented with hydrogen bonds (long-dashed lines) to two water molecules on the mica surface. (c) The movement of the silica complex across the mica surface in response to a chemical potential gradient is envisaged to occur by the transfer of hydrogen bonds, between the silica group and the oriented water molecules, from one water molecule to the next. The activation energy for such a mechanism of diffusion would thus be relatively low, and diffusion would involve two-dimensional movement only.

## DEFORMATION IN EOCENE GREYWACKES

Overlying the Eocene conglomerates referred to above is a thick flysch sequence (Barbier 1963). The greywacke sandstones consist largely of quartz and feldspar grains; a small proportion of carbonaceous material and of rock fragments is present. The sandstones have been strongly and penetratively deformed, particularly in the lower part of the sequence, and this produced grain shape fabrics. In thin section, the sandstones are seen to have deformed by incongruent pressure solution. The following observations have been made:

(i) detrital feldspars (oligoclase, albite antiperthite, orthoclase perthite, microcline) show marginal pressure solution (Figs. 2j and 3e);

(ii) detrital feldspars have been variably replaced by ferroan calcite, which may also show pressure solution at grain margins (Figs. 2j and 3e) and

(iii) intergrowths of white mica and quartz form oriented pressure shadow overgrowths, commonly on detrital quartz grains, but also on some detrital feldspar grains (Figs. 2k and 3b & f).

Thus, deformation by pressure solution proceeded via a metamorphic reaction involving the solution of feldspar and the precipitation of mica. The possible nature of this reaction is now explored. Dissolution of detrital feldspar may be written as follows:

$$\begin{aligned} KAlSi_3O_8 + 8H_2O &\rightarrow K^+ + Al(OH)_4^- + 3H_4SiO_4 \\ NaAlSi_3O_8 + 8H_2O &\rightarrow Na^+ + Al(OH)_4^- + 3H_4SiO_4 \\ CaAl_2Si_2O_8 + 8H_2O &\rightarrow Ca^{2+} + 2Al(OH)_4^- + 2HSiO_4^-. \end{aligned} \quad (1)$$

The aluminium complex $Al(OH)_4^-$ is used throughout because equilibrium calculations show that of the three common aluminium ions ($Al^{3+}$, $Al(OH)^{2+}$, $Al(OH)_4^-$), the latter is the most abundant aqueous species above a pH of 4.3, 3.3 and 2.1 at temperatures of 100, 200 and 300°C, respectively (Helgeson 1969). Precipitation of muscovite occurs when its solubility product, represented by the following, is exceeded:

$$KAl_3Si_3O_{10}(OH)_2 + 12H_2O \rightleftharpoons K^+ + 3Al(OH)_4^- + 3H_4SiO_4 + 2H^+. \quad (2)$$

Aluminium is generally considered to be conserved in metamorphic reactions (e.g. Carmichael 1969), and reactions can be written around this constraint. Helgeson (1974, 1979) states that local equilibrium between feldspar and an aqueous solution is maintained by hydrolysis at the feldspar surface, and that reaction occurs stoichiometrically. Solid state diffusion in the feldspar lattice and differential abstraction of diffusing atoms at the feldspar surface is ruled out (Helgeson 1974). Reactions may have to be balanced by recourse to external sources or sinks for some ions; it is commonly believed that ions such as $K^+$, $Na^+$ and $Ca^{2+}$ are present and available in the aqueous fluid of low grade metamorphic rocks (Helgeson 1967).

As with congruent pressure solution, diffusion during incongruent pressure solution occurs in response to gradients in chemical potential set up by stress variation around grain boundaries. Local equilibrium between solid and fluid is maintained, the fluid phase remains saturated with respect to quartz, and a local equilibrium metamorphic assemblage is established. Dissolving feldspar produces K, Al and Si species in the ratio 1/1/3, whilst precipitating mica removes them in the ratio 0.3/1/1. Thus dissolved aluminium is consumed at a greater rate than dissolved potassium. Feldspar continues to dissolve to maintain the Al concentration, and the concentrations of alkali and silica in local equilibrium are increased. Precipitation of quartz with mica in the pressure shadow areas (where the chemical potential of silica in the fluid in local equilibrium with quartz is lowest) continually removes silica released by feldspar dissolution, and further promotes this process to maintain the local equilibrium value of the feldspar solubility product.

The diffusion of alkali and aluminium in the ratio 1/3 to form the mica overgrowth raises the problem that electrical neutrality is not maintained. To do this, reaction (2) above incorporated $H^+$. It is suggested that the observed replacement of feldspar by calcite is an important and linked part of the incongruent pressure solution process, enabling it to proceed with electrical neutrality. Precipitation of calcite occurs as part of a series of aqueous carbonate equilibria, as follows:

$$C + O_2 \rightleftharpoons CO_2 \overset{+H_2O}{\rightleftharpoons} H_2CO_3 \rightleftharpoons HCO_3^- + H^+$$

$$\rightleftharpoons CO_3^{2-} + 2H^+ \overset{+Ca^{2+}}{\rightleftharpoons} CaCO_3 + 2H^+. \quad (3)$$

The source of $CO_2$ is possibly the oxidation of carbonaceous material in the sandstones. If diffusion of the aluminium ion to the mica precipitation sites occurs in conjunction with diffusion of the hydrogen ions made available, electrical neutrality is maintained. The following then expresses the overall reaction where feldspar is dissolved along its margins and partly replaced by calcite,

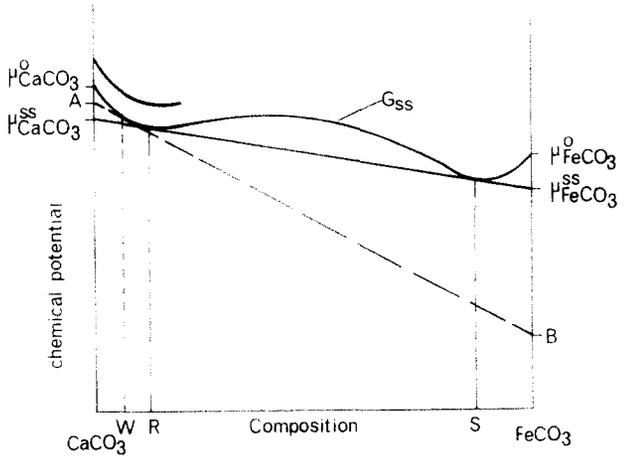


Fig. 5. Schematic G–X plot for the calcite–siderite system based on the regular solution model. The solid line tangent to the solid solution free energy curve $G_{ss}$ defines the limits of miscibility at the compositions R and S. The dashed line tangent AB derives the chemical potential of $CaCO_3$ and $FeCO_3$ in the solid solution of composition W, relative to the potentials of the pure phases ($\mu^o$).

and the silica released is precipitated with mica in the pressure shadow overgrowth:

$$4 \text{ feldspar} + 3Ca^{2+} + 3HCO_3^- \rightarrow 3 \text{ calcite} + \tfrac{4}{3}\text{mica} + 8 \text{ quartz} + \tfrac{2}{3}H^+ + \tfrac{8}{3}K^+. \quad (4)$$

This reaction would result in pressure shadows containing approximately equal volumes of mica and quartz. The intergrowths in the pressure shadows are generally too fine to enable accurate modal estimates to be made, but a one to one mixture by volume appears to be approximately correct. However, the amount of feldspar replaced by calcite can be measured more accurately. The volume ratio predicted by the reaction of this calcite to the total pressure shadow overgrowth is 1/2.7. Measurements from single thin sections fall in the range 1/2.5 to 1/3.0. It is suggested that reaction (4) above provides a realistic description of the incongruent pressure solution mechanism, and shows how metamorphic processes may be coupled during pressure solution.

## DISCUSSION

In the foregoing account petrographic data have been used as a basis of interpreting the mechanism of deformation in a variety of different rock types within a thrust zone. There appears to be a great variation in the mechanism by which the rocks deformed, and in this section some possible causes of this variation are investigated. Firstly, it is worthwhile listing those variables that may have a significant effect on the mechanism of deformation. These are mean stress (pressure), temperature, stress difference, strain rate, fluid pressure, grain size, fluid composition, activities of species in solution in the fluid phase and in local equilibrium with the mineral assemblage of the rock. In a sense, this is a conventional structural–metamorphic problem except that to date, deformation mechanisms have only been evaluated in terms of temperature, stress difference, grain size and strain rate (e.g. Rutter 1976, White 1976). In this account, variations in deformation mechanism are discussed in relation to variations in lithology. The question arises as to whether the deformation mechanism depends upon structural position within the thrust pile. On the basis of a progressive development of a thrust belt towards the foreland (Dahlstrom 1970, see Frisch 1979 on the Alps), the deformation accompanying formation of the Ultra-dauphinois thrust slices discussed here would have taken place beneath the previously overthrust internal nappes. Thus the rocks described here would have been subjected to a similar depth of burial and therefore mean pressure at the time of their deformation. It is expected that changes in deformation mechanism related to variations in structural position will occur on a larger scale than that of the area studied here, e.g. from one regional nappe structure to another. Strain rate variations through one developing thrust sheet may be recorded as variations in deformation mechanism. Though this cause cannot be clearly isolated in the area under discussion, Ramsay (1981) has described such a variation in the Morcles nappe, Switzerland.

Emphasis is given here to the chemical control of the deformation mechanism through lithological and mineralogical variations. Firstly, it has been found that the Triassic dolomites remain relatively undeformed and are not affected by pressure solution, whereas adjacent Jurassic calcareous rocks are strongly deformed by pressure solution. Clearly, at the stress and temperature levels in existence at the time of deformation, grain boundary stress gradients sufficient to give rise to appreciable diffusion of the components of dolomite did not exist. It may be that the grain boundary structure in the relatively clean and pure dolomites slows considerably the rate of diffusion. It is also likely that the rate of diffusion of the magnesium ion is less than that of the calcium ion because of the difference in solvated ion radii (3.8 Å and 3.4 Å, respectively). The purity of the rock is also significant to the deformation of the calcareous rocks where there is a range from limestones with a low mud content through to calcareous shales. Firstly, it has been argued that the presence of a preferred orientation of mica considerably facilitates diffusion through surface effects. Secondly, the metamorphic reactions by which the clay mineral assemblage evolves (see Beach 1979) will cause loss of grain boundary structure at all points where the reaction is occurring, facilitating both diffusion and grain boundary sliding.

It appears that the ability of a mineral to show small changes in composition by solid solution may significantly affect the amount of deformation by pressure solution. This is based on the observation that considerable solution of calcite and precipitation of ferroan-calcite has occurred in many of the deformed Jurassic rocks, but that those which show development of the mylonitic structure during deformation have no ferroan-calcite amongst the recrystallised grains. Clearly it is not possible to rule out the effect of stress difference/strain rate in changing the deformation mechanism. However, rocks deformed by pressure solution of calcite and by grain size reduction occur in a structurally continuous succession for which there is no field evidence in support of a different structural history for each rock group. The availability of iron in solution during pressure solution (considered to be derived from the breakdown of siderite grains) is thought to affect significantly the extent to which a rock will deform by pressure solution. This can be understood by reference to a simplified phase diagram for calcite–siderite (Fig. 5) based on a regular solution model of solid–solution (Wood & Fraser 1976), showing the variation of chemical potential with composition along the curve marked $G_{ss}$. The line which is tangent to both portions of the inflexed curve defines the limits of the symmetrical miscibility gap at compositions R and S for coexisting calcite and siderite. The chemical potential of $CaCO_3$ in the calcite is the same as that in the siderite, and similarly for the $FeCO_3$ component. Another tangent is drawn on Fig. 5 for composition W, a ferroan-calcite with the chemical potential of the $CaCO_3$ component being given by A and that of the $FeCO_3$ component by B. Now consider a rock consisting of grains of pure calcite under a differential stress. There will be a variation in the chemical

potential of $CaCO_3$ in solution in local equilibrium with the grains, around the value $\mu^0_{CaCO_3}$ shown in Fig. 5. Higher values will exist at points of high stress, and lower values at points of low stress. For the example where iron is available in solution, pure calcite is in local equilibrium with the grain boundary fluid at points of high stress where solution occurs, and ferroan-calcite is in local equilibrium with the grain boundary fluid at points of low stress where precipitation occurs. The phase diagram (Fig. 5) should be redrawn, with a $G_{ss}$ curve for high stress locations positioned above that shown, and another for low stress locations, positioned below the one shown. Thus a stressed aggregate of pure calcite grains will show a variation in chemical potential $\mu^0_{CaCO_3}$, while for the same stress difference, an aggregate of calcite grains with iron available in solution will show a much greater variation in chemical potential from $\mu^0_{CaCO_3}$, at high stress points to $\mu^{ss}_{CaCO_3}$ at points of low stress where ferroan calcite is being precipitated. On Fig. 5, if the complete $G_{ss}$ curve shown corresponds to points of low stress, and the partial curve shown above this to points of high stress, then the increase in the magnitude of the chemical potential gradient for systems dissolving calcite and precipitating ferroan-calcite can be qualitatively appreciated.

The chemical control on the extent to which deformation by pressure solution occurs is also seen in the deformed greywackes described where a metamorphic reaction is part of the pressure solution mechanism. The full reaction (4) which describes the solution of feldspar at high stress points and the precipitation of mica and quartz at low stress points is complex because calcite precipitation also occurs. The effect of local microchemical changes in the grain boundary fluid can be explored using equilibrium constants for reactions. No data is available for the reaction (4), but for a simplified muscovite–feldspar reaction

$$3KAlSi_3O_8 + 2H^+ \rightleftharpoons KAl_3Si_3O_{10}(OH)_2 + 6SiO_2 + 2K^+ \quad (5)$$

equilibrium constants up to 300°C have been tabulated by Helgeson (1967). The equilibrium of the reaction will be affected by stress variation on the feldspar grains, and the activities of species in solution in local equilibrium with dissolving feldspar and with precipitating muscovite and quartz. The activities of $H^+$ and $K^+$ are important in reaction (5). As an example, the activity of $H^+$ may be held constant at, say, $10^{-7}$, and the difference in chemical potentials between reactants and products of reaction (5) calculated for a range in the activity of $K^+$ for a given temperature. The results are shown in Fig. 6. It can be seen that either external buffering of the activity of $K^+$ away from equilibrium, or departures in the activity of $K^+$, as caused by local stress variation from one grain to another, from equilibrium values, will ensure that pressure solution occurs via the metamorphic reaction (i.e. solution of feldspar at high stress points, deposition of muscovite at low stress points) because this is where the largest chemical potential gradients exists.

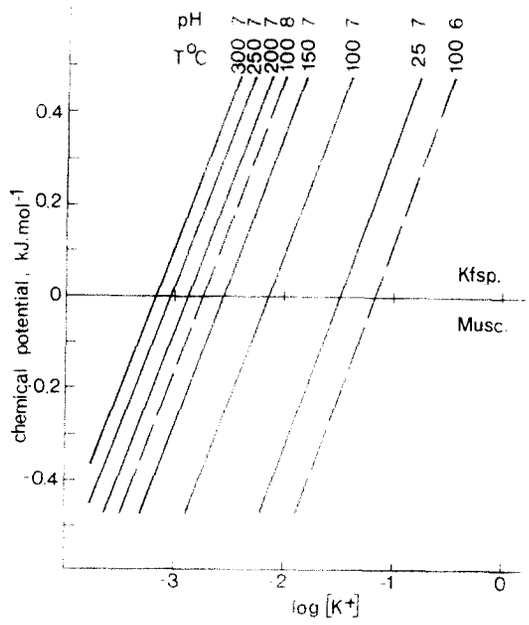


Fig. 6. Magnitude of the chemical potential difference driving the reaction K-feldspar to muscovite as a function of activity of $K^+$, at constant activity of $H^+$ of $10^{-7}$, and with unit activity for all solid phases, in the temperature range 25–300°C. For comparison, the dashed lines are at $H^+$ activities of $10^{-6}$ and $10^{-8}$, at 100°C. Based on Helgeson's (1967) one atmosphere standard state equilibrium constants.

In conclusion, it is suggested that local chemical conditions in a deforming rock may determine whether or not a metamorphic reaction or a solid-solution compositional change can occur, and therefore whether or not these can be utilised as part of the pressure solution mechanism. In their absence, chemical potential gradients may be too small to allow pressure solution to constitute a significant part of the overall rock deformation. The chemical control of the deformation mechanism may be just as important as the stress–grain size–temperature control discussed by Rutter (1976) and White (1976) in their deformation mechanism maps.

*Acknowledgements*—This work was supported by NERC grant GR3/3472, which is gratefully acknowledged. I would like to thank P. Vialon, J. P. Gratier and their colleagues at Grenoble University for their help whilst I was working on this project. I would like to thank J. Lynch for his help with preparing the figures.

## REFERENCES

Barbier, R. 1963. La tectonique de la zone ultradauphinoise du NE du Pelvoux. *Trav. Lab. Géol. Grenoble* **39**, 239–246.

Beach, A. 1979. Pressure solution as a metamorphic process in deformed terrigenous sedimentary rocks. *Lithos* **12**, 51–58.

Beach, A. 1981a. Thrust structures in the eastern Dauphinois zone, French Alps. *J. Struct. Geol.* **3**, 299–308.

Beach, A. 1981b. Cover-basement relations along the northern margin of the Pelvoux massif, French Alps. *Eclog. geol. Helv.* **74**, 471–479.

Beach, A. 1981c. Some observations on the development of thrust faults in the Ultradauphinois Zone, French Alps. In: *Thrust and Nappe Tectonics* (edited by McClay, K. R. & Price, N. J.). Geol. Soc. Lond. Sp. Publ. **9**, 329–334.

Bernard, D. 1978. Microthermométrie des inclusions fluides de cristaux syncinématiques: application à la couverture sédimentaire du nord Pelvoux. Thèse 3ème cycle. Univ. Grenoble.

Bernard, D., Gratier, J. P. & Pecher, A. 1977. Application de la microthermométrie des inclusions fluides des cristaux syncinématiques à un problème tectonique. *C. r. somm. séanc. Soc. géol. Fr.* **5**, 284–288.

Borradaile, G. J. 1981. Particulate flow of rock and the formation of cleavage. *Tectonophysics* **72**, 305–321.

Bravard, C. & Gidon, M. 1979. La structure du revers oriental du Massif du Pelvoux : observations et interprétations nouvelles. *Géol. Alpine* **55**, 23–33.

Carmichael, D. M. 1969. On the mechanism of prograde metamorphic reactions in quartz bearing pelites. *Contr. Miner. Petrol.* **20**, 244–267.

Dahlstrom, C. D. A. 1970. Structural geology in the eastern margin of the Canadian Rockies. *Bull. Can. Petrol. Geol.* **18**, 332–406.

Debelmas, J. & Kerckhove, C. 1980. Les Alpes franco-italiennes. *Géol. Alpine* **56**, 21–58.

Debelmas, J. & Lemoine, M. 1970. The western Alps: paleogeography and structure. *Earth Sci. Rev.* **6**, 221–256.

Durney, D. W. 1972. Solution transfer, an important geological deformation mechanism. *Nature, Lond.* **235**, 315–317.

Durney, D. W. 1976. Pressure solution and crystalline deformation. *Phil. Trans. R. Soc.* **A283**, 229–240.

Fisher, G. W. 1978. Rate laws in metamorphism. *Geochim. cosmochim. Acta* **42**, 1035–1050.

Fisher, G. W. & Elliott, D. 1974. Criteria for quasi-steady diffusion and local equilibrium in metamorphism. In: *Geochemical Transport and Kinetics* (edited by Hofmann, A. W. *et al.*). Carnegie Inst. Publ. **634**, 231–241.

Frisch, W. 1979. Tectonic progradation and plate tectonic evolution of the Alps. *Tectonophysics* **60**, 121–139.

Gratier, J. P. 1979. Mise en évidence de relations entre changement de composition chimique et intensité de déformation dans les roches à schistosité. *Bull. Soc. géol. Fr.*, 7 *Ser.* **21**, 95–104.

Heald, M. T. 1955. Stylolites in sandstones. *J. Geol.* **63**, 16–30.

Heald, M. T. 1959. Significance of stylolites in permeable sandstones. *J. sedim. Petrol.* **29**, 251–253.

Helgeson, H. C. 1967. Solution chemistry and metamorphism. In: *Researches in Geochemistry* (edited by Abelson, P. H.) vol. II. Wiley, 363–404.

Helgeson, H. C. 1969. Thermodynamics of hydrothermal systems at elevated temperatures and pressures. *Am. J. Sci.* **267**, 729–804.

Helgeson, H. C. 1974. Chemical interaction of feldspars and aqueous solutions. In: *The Feldspars* (edited by MacKenzie, W. S. & Zussman, J.). Manchester Univ. Press 184–217.

Helgeson, H. C. 1979. Mass transfer among minerals and hydrothermal solutions. In: *Geochemistry of Hydrothermal Ore Deposits* (edited by Barnes, H. L.) 2nd edition. Wiley, New York, 568–610.

Higgins, M. W. 1971. Cataclastic rocks. *Prof. Pap. U.S. geol. Surv.* 687, 1–97.

Kerrich, R. 1977. An historical review and synthesis of research on pressure solution. *Zentbl. Miner. Geol. Paläont.*, 512–550.

Kerrich, R., Beckinsale, R. D. & Durham, J. J. 1977. The transition between deformation regimes dominated by intercrystalline diffusion and intracrystalline creep evaluated by oxygen isotope thermometry. *Tectonophysics* **38**, 241–257.

Lacy, E. D. 1965. Factors in the study of metamorphic reaction rates. In: *Controls of Metamorphism*, (edited by Pitcher, W. S. & Flinn, G. W.) Geol. J. Spec. Publ. **1**, 140–154.

Lisle, R. J. 1977. Estimation of the tectonic strain ratio from the mean shape of deformed elliptical particles. *Geologie Mijnb.* **56**, 140–144.

McClay, K. R. 1977. Pressure solution and Coble creep in rocks and minerals: a review. *J. geol. Soc. Lond.* **134**, 57–70.

McLean, D. 1965. The science of metamorphism in metals. In: *Controls of Metamorphism*, (edited by Pitcher, W. S. & Flinn, G. W.) Geol. Jour. Spec. Publ. **1**, 103–118.

Paterson, M. S. 1973. Nonhydrostatic thermodynamics and its geologic application. *Rev. Geophys. Space Phys.* **11**, 355–390.

Ramsay, J. G. 1981. Tectonics of the Helvetic nappes. In: *Thrust and Nappe Tectonics* (edited by McClay, K. R. & Price, N. J.) Geol. Soc. Lond. Spec. Publ. **9**, 293–309.

Robin, P.-Y. F. 1979. Theory of metamorphic segregation and related processes. *Geochim. cosmochim. Acta* **43**, 1587–1600.

Rutter, E. H. 1976. The kinetics of rock deformation by pressure solution. *Phil. Trans. R. Soc.* **A283**, 203–219.

Schmid, S. M., Casey, M. & Starkey, J. 1981. The microfabric of calcite tectonites from the Helvetic nappes. In: *Thrust and Nappe Tectonics* (edited by McClay, K. R. & Price, N. J.) Geol. Soc. Lond. Spec. Publ. **9**, 151–158.

Warrak, M. 1974. The petrography and origin of dedolomitized, veined or brecciated carbonate rocks, the cornieules, in the Fréjus region, French Alps. *J. geol. Soc. Lond.* **130**, 229–247.

White, S. 1976. The effects of strain on the microstructures, fabrics and deformation mechanisms in quartzites. *Phil. Trans. R. Soc.* **A283**, 69–86.

Wood, B. J. & Fraser, D. G. 1976. *Elementary Thermodynamics for Geologists*. Oxford University Press, Oxford.